

Universal scaling of spontaneous imbibition for water-wet systems

K. S. Schmid¹ and S. Geiger¹

Received 28 October 2011; revised 17 January 2012; accepted 24 January 2012; published 7 March 2012.

[1] Spontaneous, counter-current imbibition (SI) is a key mechanism in many multiphase flow processes, such as cleanup of nonaqueous phase liquids (NAPLs), bioremediation, or CO₂ storage. For interpreting and upscaling laboratory SI data, and modeling and prediction purposes, scaling groups are an essential tool. The question of how to formulate a general scaling group has been debated for over 90 years. Here we propose the first scaling group that incorporates the influence of all parameters on SI that are present in the two-phase Darcy model. The group is derived rigorously from the only known exact analytical solution for spontaneous imbibition by relating the cumulative water phase imbibed to the normalized pore volume. We show the validity of the group by applying it to 42 published SI studies for water-oil and water-air experiments, for a wide range of viscosity ratios, different materials, different initial water saturations, and different length-scales. In all cases, water was the wetting phase. Our group serves as a “master equation” whose generality allows the rigorous prediction of the validity of a large number of specialized scaling groups proposed during the last 90 years. Furthermore, our results give strong evidence that the Darcy model is suitable for describing SI, and that including dynamic effects in capillary pressure is not necessary for counter-current SI, contrary to what has been hypothesized. Two key applications of the group are discussed: First, the group can serve as the long sought after general transfer rate for imbibition used in dual-porosity models. Second, it is the so far missing proportionality constant in imbibition-germination models for plant seeds.

Citation: Schmid, K. S., and S. Geiger (2012), Universal scaling of spontaneous imbibition for water-wet systems, *Water Resour. Res.*, 48, W03507, doi:10.1029/2011WR011566.

1. Introduction

[2] Spontaneous imbibition (SI) (Figure 1) occurs if a wetting fluid (like water or brine) spontaneously enters a porous medium, and displaces a nonwetting fluid (like oil, air, nonaqueous phase liquids (NAPL), or CO₂), driven by capillary forces only. It is a process that is of crucial importance for many processes ranging from groundwater contamination by NAPL transport [Brusseau, 1992], CO₂ storage by capillary trapping [Bickle, 2009; Juanes et al., 2006; Pentland et al., 2011], steam migration in high-enthalpy geothermal systems [Li and Horne, 2009], the mechanical stability and distribution of gas-hydrate bearing sediments [Clennell et al., 1999; Anderson et al., 2009], trapping of CO₂ in coal seams and generation of methane [Chaturvedi et al., 2009], improved oil recovery from the world’s largest remaining oil reserves [Morrow and Mason, 2001], evaluating the wettability of a rock [Jadhunandan and Morrow, 1991; Marmur, 2003] and even many other processes not linked with hydrogeological applications at all [Alava et al., 2004; Finch-Savage et al., 2005].

[3] The advancing displacement front of the wetting phase during SI shows some “roughness” due to heterogeneities at

the pore scale. While it is well known from statistical physics [Alava et al., 2004] that the averaged position of the rough displacement front and the recovery R of the displaced fluid scales with \sqrt{t} in time, as predicted by the Lucas-Washburn equation [Lucas, 1918; Washburn, 1921], the properties of this scaling are still unknown.

[4] Scaling groups are used to characterize the influence of key parameters on SI other than time, and are essential in any context where SI needs to be understood and described. For example, they are a central tool for interpretation of laboratory data and upscaling them to field conditions [Morrow and Mason, 2001], they lie at the heart of modeling and simulating multiphase flow in different scenarios like flow in heterogeneous, fractured aquifers and reservoirs [Barenblatt et al., 1960; Warren and Root, 1963; Di Donato and Blunt, 2004], water uptake in plant seeds [Finch-Savage et al., 2005], or are needed as a starting point for evaluating the feasibility of water injection in high-enthalpy geothermal reservoirs [Li and Horne, 2009]. Despite this immense practical importance, however, and although the research on SI and scaling groups spans more than 90 years [Lucas, 1918; Washburn, 1921], not even apparently simple questions—like that of the influence of viscosity ratios on SI—have been resolved satisfactorily because of the strong nonlinearities in the capillary-hydraulic properties [Morrow and Mason, 2001; Marmur, 2003; Mason et al., 2010].

[5] Scaling groups for SI in realistic porous media (Table 1) have been derived mainly in two ways. Either a

¹Institute of Petroleum Engineering, Heriot-Watt University, Edinburgh, UK.

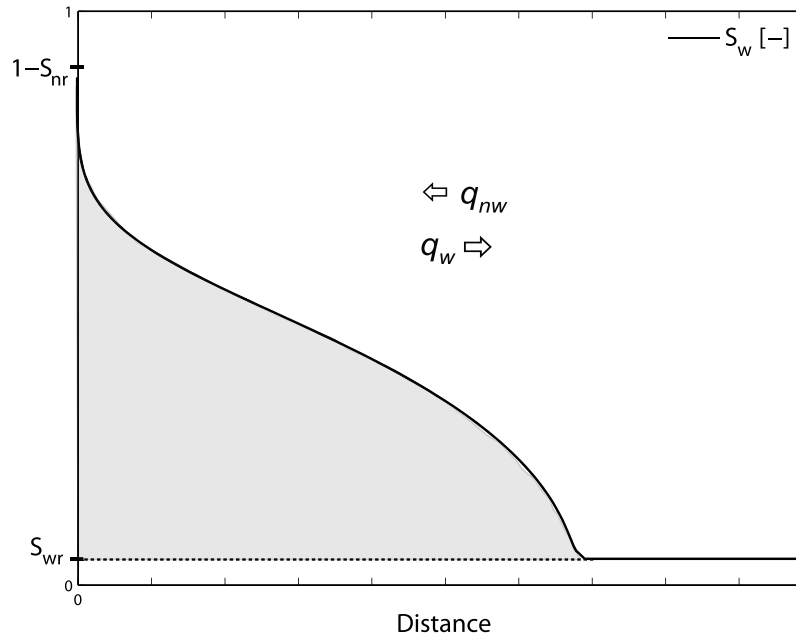


Figure 1. Schematic representation of countercurrent SI. The water phase is imbibed from the left and the oil phase moves into opposite direction. If an analytical solution for the saturation profile $S_w(x, t)$ is known, then the analytical expression for the cumulative water imbibed $Q_w(t)$ (shaded region) can be related to the effective pore volume $\phi \cdot L_c$ to obtain a scaling group as $t_d = \left[\frac{Q_w(t)}{\phi \cdot L_c} \right]^2$.

curve was fitted against a large body of experimental data and a single parameter was varied to analyze its influence, or simplifying assumptions on the form of the hydraulic diffusivity function in Darcy’s equation [Gummerson *et al.*, 1979; McWhorter and Sunada, 1990; Schmid *et al.*, 2011] (Table 2) were employed from which new specialized analytical solutions were derived that then served as basis for introducing specific scaling groups. Both approaches yield groups whose applicability is strongly restricted. On the one hand, a general theoretical understanding on why a certain group works and when it would fail is left unanswered. On the other hand, the incorporation of three key aspects into scaling groups remains open, which play a central role in many practical applications.

[6] First, the mobility of the fluids is governed by the relative permeability of one phase to the other and is weighted by their respective viscosities. It is unclear [Morrow and Mason, 2001; Mason *et al.*, 2010] how this weighting should depend on the viscosity ratio such that in the limit of an inviscid nonwetting phase the Lucas-Washburn equation is obtained [Lucas, 1918; Washburn, 1921], and how a single relative permeability value should be chosen such that it characterizes the strong nonlinear dependence on the wetting phase volume fraction over the whole saturation range (Figure 2).

[7] Second, if the porous medium initially contains a wetting phase, competition occurs between the low capillary pressure force and the high phase mobilities (Figure 2)

Table 1. Lucas-Washburn Scaling and Some of the Recently Defined t_d ^a

Author	Dimensionless Time	Proportionality Constant
Lucas [1918]; Washburn [1921]	$t_d \propto \frac{1}{2L_c^2} r \frac{\sigma}{\mu_w} t$	$c \approx \int_{S_0}^{S_{BC}} \frac{(S_w - S_0)k_{rw}J'(S_w)}{F(S_w)} dS_w$
Rapoport [1955], Mattax and KYTE [1962]	$t_d \propto \frac{1}{L_c^2} \sqrt{\frac{K}{\phi}} \sqrt{\frac{\sigma}{\mu_w}} t$	$c = \int_{S_0}^{S_{BC}} \frac{(S_w - S_0)\sqrt{k_{rw}k_{ro}J'(S_w)}}{F(S_w)} dS_w$
Ma <i>et al.</i> [1997]	$t_d \propto \frac{1}{L_c^2} \sqrt{\frac{K}{\phi}} \sqrt{\frac{\sigma}{\mu_w \mu_n}} t$	$c \approx \int_{S_0}^{S_{BC}} \frac{(S_w - S_0)\sqrt{k_{ro}k_{rw}J'(S_w)}}{F(S_w)} dS_w$
Zhou <i>et al.</i> [2002]	$t_d \propto \frac{1}{L_c^2} \sqrt{\frac{K}{\phi}} \sigma \left(\frac{\lambda_w \lambda_o}{\lambda_r} \right)^* t$	$c \approx \int_{S_0}^{S_{BC}} \frac{(S_w - S_0)J'(S_w)}{F(S_w)} dS_w$
Tavassoli <i>et al.</i> [2005a]	$t_d \propto \frac{1}{L_c^2} \sqrt{\frac{K}{\phi}} \sigma \left(\frac{\lambda_w \lambda_o}{\lambda_r} \right)^* J'^* t$	$c \approx \int_{S_0}^{S_{BC}} \frac{(S_w - S_0)}{F(S_w)} dS_w$
Li and Horne [2006]	$t_d \propto \frac{1}{L_c^2} \sqrt{\frac{K}{\phi}} \sigma \left(\frac{\lambda_w \lambda_o}{\lambda_r} \right)^* J^* \cdot (S_{BC} - S_0) t$	$c \approx \frac{1}{F(S_w)}$
This work	$t_d \propto \left(\frac{2A}{\phi L_c} \right)^2 t$	$c = 1$

^aCharacteristic values are denoted by (*). It is now apparent, how previous authors (unknowingly) have derived successively better expressions for t_d by giving approximations to the integral in equation (3). A specific t_d will give a good scaling if c is the same for the different data sets, and thus c can be used to predict the validity of a special scaling group (Figure 4).

Table 2. Previously Derived Analytical Solutions for Two-Phase Flow With Capillary Effects^a

Author and Year	Assumption
<i>Fokas and Yortsos</i> [1982], <i>Yortsos and Fokas</i> [1983], <i>Philip</i> [1960], <i>Chen</i> [1988], <i>Ruth and Arthur</i> [2011], <i>Wu and Pan</i> [2003], <i>Kashchiev and Firoozabadi</i> [2002]	Specific functional forms for k_{rw} , k_{ro} , p_c
<i>Li et al.</i> [2003]	Steady-state, i.e., $\frac{\partial S_w}{\partial t} = 0$
<i>Barenblatt et al.</i> [1990], <i>Zimmerman and Bodvarsson</i> [1989], <i>Tavassoli et al.</i> [2005b], <i>Tavassoli et al.</i> [2005a], <i>Mirzaei-Paiaman et al.</i> [2011]	Piston-like displacement, i.e., $F(x, t) = \frac{q_w(x^*, t)}{q_w(0, t)}$
<i>Handy</i> [1960], <i>Chen et al.</i> [1995], <i>Sanchez Bujanos et al.</i> [1998], <i>Rangel-German and Kovscek</i> [2002]	Approximate solution for the weak form
<i>Ruth et al.</i> [2007]	Existence of an equivalent constant capillary diffusion coefficient
<i>Cil and Reis</i> [1996], <i>Reis and Cil</i> [1993]	Self-similarity behaves according to to specific functional form
<i>Rasmussen and Civan</i> [1998], <i>Civan and Rasmussen</i> [2001]	Linear capillary pressure, i.e., $\frac{dp_c}{dx} = \frac{p_c(S_0)}{L}$
<i>Zimmerman and Bodvarsson</i> [1991]	Asymptotic approximation of laplace transformation for S_w , Piecewise linear S_w profile

^aTo resolve the influence of capillarity, all of them need to employ additional, nonessential assumptions that restrict their applicability. On contrary, it can be shown [Schmid et al., 2011] that the solution given in the work of *McWhorter and Sunada* [1990] is general. It can be viewed as the Buckley-Leverett analog for countercurrent SI (see section 2.2). This makes the derivation of further specific solutions unnecessary.

[Parrish and Leopold, 1977; Morrow and Mason, 2001]. So far, this effect has only been characterized for cases where the ratio of nonwetting to wetting phase viscosity is close to one, and if the capillary pressure and the wetting behavior can be characterized by a single value [Li and Horne, 2006] which is unlikely in realistic porous media [Valvatne and Blunt, 2004] (Figure 2).

[8] Third, capillary pressure curves and the phase mobilities not only depend on the fluids, but also on the geometry of the pore structure, and thus are different for different materials [Valvatne and Blunt, 2004] (Figure 2). Up to now, however, scaling groups try to characterize the influence of capillary pressure and wetting by some single value that is representative of the entire porous medium [Tavassoli et al., 2005a; Li and Horne, 2006; Marmur, 2003].

[9] In addition to these three practical issues, the very theoretical framework for describing SI has been the center of debate in physics and engineering. It has been proposed that the classical Darcy approach [Bear, 1972] is unsuitable for SI and should be replaced by a model that incorporates dynamic changes in capillary pressure (for recent overviews, see Hall [2007], Bottero et al. [2011], Goel and O'Carroll [2011], Manthey et al. [2008]).

[10] In the following, for the first time all three practical aspects will be accounted for. We also discuss the validity of the classical Darcy description for describing SI.

[11] The remainder of our paper is structured as follows: First, the problem formulation and an exact analytical solution for countercurrent imbibition are introduced. Until recently [Schmid et al., 2011], the derivations of analytical solutions for capillary dominated two-phase flow has been the matter of intensive research (Table 2). We rigorously derive our scaling group from the only known general analytical solution for imbibition [Schmid et al., 2011; McWhorter and Sunada, 1990], which can be viewed as the capillary counterpart to the Buckley-Leverett solution for viscous dominated flow [Buckley and Leverett, 1942]. No assumptions other than those needed for Darcys model are made. No fitting parameters are introduced. In section 3.1 we show the validity of our scaling group by correlating 42 published imbibition studies that vary all key parameters, namely material and capillary-hydraulic properties, viscosity

ratios, initial water saturation, and characteristic lengths (Table 3). We then show that our group is a “master equation” for scaling SI, which contains many of the previously defined groups as special cases (Table 1), and demonstrate how the generality of our approach allows the prediction of the validity range of specialized groups (Table 1). This is the first predictive theory for evaluating scaling groups. We also will give strong evidence that the classical Darcy description for SI is appropriate. The paper is finished with some conclusions.

2. Model Formulation, Exact Solution and the Universal Scaling Group

2.1. Problem Formulation

[12] Conservation of mass for two immiscible, incompressible phases at constant temperature through a homogeneous, one-dimensional, rigid, horizontal, i.e., gravity is absent, porous medium leads to the following equation [Bear, 1972]

$$\phi \frac{\partial S_w}{\partial t} = -\frac{\partial}{\partial t}(q_w), \quad S_w + S_n = 1, \quad (1)$$

where S_w is the water phase saturation, S_n is the nonaqueous phase saturation, and ϕ is the porosity. We assume that the volume flux of the wetting and nonwetting phase, q_w and q_o , respectively, can be described by the extended Darcy equation [Muskat, 1949], which describes the volume flux due to a gradient in the phase pressures p_w and p_{nw} :

$$q_w = -K \frac{k_{rw}}{\mu_w} \nabla p_w, \quad q_{nw} = -K \frac{k_{rn}}{\mu_n} \nabla p_{nw}. \quad (2)$$

Here K is the absolute permeability, μ_w is the viscosity of the wetting phase, μ_n is the viscosity of the nonwetting phase, and k_{rn} and k_{rw} are the relative permeability of the nonwetting phase and the wetting phase, respectively. The relative permeabilities describe the impairment of the one fluid phase by the other. We furthermore assume that the two-phase pressures p_w and p_{nw} are related through the

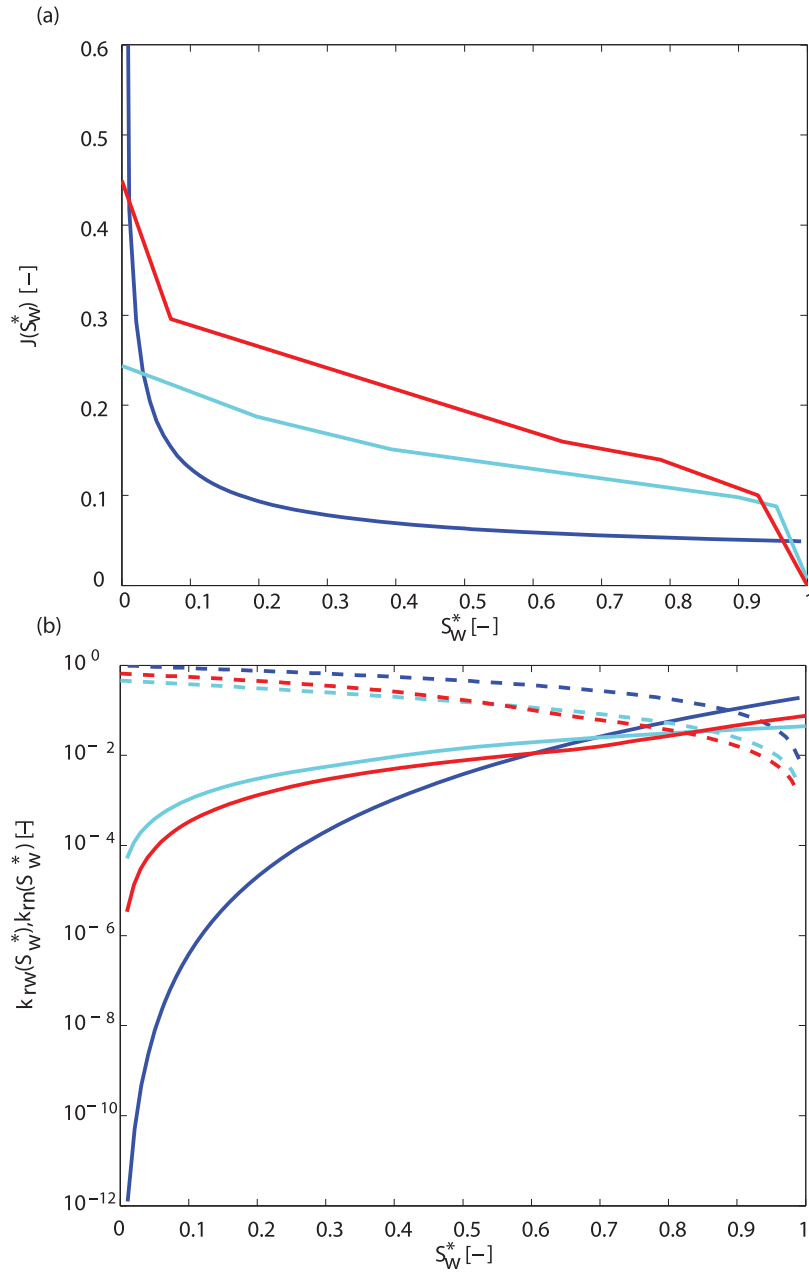


Figure 2. Capillary-hydraulic properties versus saturation. Capillary-hydraulic properties of Berea sandstone and a synthetic porous material (blue) [Valvatne and Blunt, 2004] from pore-scale predictions, a history match that assumes a Darcy model for sandstone (cyan) [Bourbiaux and Kalaydjian, 1990], and a non-Darcy-model [Schembre and Kovscek, 2006] for diatomite (red). (a) Dimensionless J function. (b) Relative permeability for the wetting (—) and nonwetting phase (---).

capillary pressure $p_c = p_{nw} - p_w$ [Bear, 1972]. Combining equations (1) and (2), we obtain [Bear, 1972]

$$\phi \frac{\partial S_w}{\partial t} = -q_t \frac{df_w}{dS_w} \frac{\partial S_w}{\partial t} + \frac{\partial}{\partial x} \left[D(S_w) \frac{\partial S_w}{\partial x} \right], \quad (3)$$

where $q_t = q_w + q_{nw}$. One can rewrite q_w as an expression of the total volume flux [McWhorter and Sunada, 1990]

$$q_w = f(S_w) q_t - D(S_w) \frac{\partial S_w}{\partial x}. \quad (4)$$

[13] We consider the boundary and initial conditions

$$\begin{aligned} S_w(x=0, t) &= S_{BC} \\ S_w(x, t=0) &= S_w(\infty, t) = S_0. \end{aligned} \quad (5)$$

[14] The functions $f(S_w)$ and $D(S_w)$ are defined as

$$f(S_w) = \left(1 + \frac{k_{rn} \mu_w}{k_w \mu_n} \right)^{-1}, \quad D(S_w) = -K \frac{k_{rn} f}{\mu_n} \frac{dp_c}{dS_w}. \quad (6)$$

Table 3. Parameter Sets Referenced in the Text and Their Corresponding References

Sample ^a	L_c [cm]	k [mD]	ϕ [–]	μ_w [Pa · s]	μ_n [Pa · s]	σ [mN/m]	S_0 [–]	A [m/\sqrt{s}]
<i>Zhang et al.</i> [1996]								
AA01	0.5364	510.8	0.218	9.67×10^{-4}	0.03782	50.62	0	7.307×10^{-6}
AA02	0.8029	498.5	0.219	9.67×10^{-4}	0.03782	50.62	0	7.287×10^{-6}
AA03	0.9723	519.8	0.222	9.67×10^{-4}	0.03782	50.62	0	7.44×10^{-6}
AA04	1.089	521.7	0.224	9.67×10^{-4}	0.03782	50.62	0	7.45×10^{-6}
AA05	1.1837	505.5	0.215	9.67×10^{-4}	0.03782	50.62	0	7.21×10^{-6}
AA06	1.3059	501.6	0.218	9.67×10^{-4}	0.03782	50.62	0	7.27×10^{-6}
BC21	6.092	481.9	0.213	9.67×10^{-4}	0.00398	47.38	0	1.25×10^{-5}
BC13	4.998	503.6	0.209	9.67×10^{-4}	0.03782	47.38	0	7.05×10^{-6}
BC22	5.687	496.8	0.208	9.67×10^{-4}	0.1563	51.77	0	4.46×10^{-6}
BD15	1.3506	523.8	0.214	9.67×10^{-4}	0.00398	47.38	0	1.28×10^{-5}
BD14	1.3506	518.9	0.218	9.67×10^{-4}	0.03782	50.62	0	7.34×10^{-6}
BD18	1.3506	509.7	0.218	9.67×10^{-4}	0.1563	51.77	0	4.65×10^{-6}
BA3	13.87	907.1	0.214	9.67×10^{-4}	0.03782	50.62	0	4.65×10^{-6}
<i>Hamon and Vidal</i> [1986]								
A10	9.7	4000	0.472	0.001	0.0115	49.0	0.189	3.36×10^{-5}
A10-20	19.7	3430	0.453	0.001	0.0115	49.0	0.187	3.1×10^{-5}
A10-30	30.0	3830	0.453	0.001	0.0115	49.0	0.151	3.18×10^{-5}
A10-40	40.0	3550	0.478	0.001	0.0115	49.0	0.172	3.33×10^{-5}
A10-85	84.7	3000	0.478	0.001	0.0115	49.0	0.164	3.13×10^{-5}
A10-VI-20	19.8	3200	0.456	0.001	0.0115	49.0	0.164	3.17×10^{-5}
A10-X-20	20.0	2300	0.458	0.001	0.0115	49.0	0.132	2.92×10^{-5}
<i>Zhou et al.</i> [2002]								
Z-2	9.5	6.1	0.72	0.001	8.4×10^{-4}	51.4	0	3.41×10^{-5}
Z-3	9.5	7.9	0.77	0.001	2.5×10^{-2}	45.7	0	1.35×10^{-5}
Z-4	9.5	2.5	0.78	0.001	8.4×10^{-4}	51.4	0	2.72×10^{-5}
Z-5	9.5	6.0	0.68	0.001	8.4×10^{-4}	51.4	0	2.86×10^{-5}
<i>Bourbiaux and Kalaydjian</i> [1990]								
GVB-3	29.0	124.0	0.233	0.0012	0.0015	35.0	0.4	1.24×10^{-5}
GVB-4	14.5	118.0	0.233	0.0012	0.0015	35.0	0.411	9.67×10^{-6}
<i>Fischer et al.</i> [2006]								
EV6-22	7.18	109.2	0.18	0.495	0.0039	28.9	0	4.29×10^{-7}
EV6-18	7.62	140.0	0.181	0.001	0.063	51.3	0	3.74×10^{-6}
EV6-21	7.7	107.3	0.187	0.0278	0.0039	34.3	0	1.86×10^{-6}
EV6-13	7.75	113.2	0.187	0.001	0.0039	50.5	0	7.48×10^{-6}
EV6-14	7.66	127.2	0.178	0.0041	0.0039	41.2	0	4.45×10^{-6}
EV6-20	7.52	132.9	0.181	0.0041	0.0633	41.7	0	2.45×10^{-6}
EV6-16	7.78	136.8	0.181	0.0278	0.0633	34.8	0	1.36×10^{-6}
EV6-23	7.36	132.1	0.179	0.0977	0.0039	31.3	0	9.92×10^{-7}
EV6-15	7.3	107.0	0.183	0.4946	0.0633	29.8	0	3.93×10^{-7}
EV6-17	7.54	128.1	0.19	0.0977	0.0633	32.1	0	8.59×10^{-7}
<i>Babadagli and Hatiboglu</i> [2007]								
F-11	10.16	500.0	0.21	0.001	1.8×10^{-5}	72.9	0	2.75×10^{-5}
F-12	15.24	500.0	0.21	0.001	1.8×10^{-5}	72.9	0	2.81×10^{-5}
F-14	10.16	500.0	0.21	0.001	1.8×10^{-5}	72.9	0	1.95×10^{-5}
F-16	5.08	500.0	0.21	0.001	1.8×10^{-5}	72.9	0	2.29×10^{-5}
F-16	10.16	500.0	0.21	0.001	1.8×10^{-5}	72.9	0	1.60×10^{-5}
F-18	15.24	500.0	0.21	0.001	1.8×10^{-5}	72.9	0	2.07×10^{-5}

^aThe porous material in the work of *Zhang et al.* [1996] *Bourbiaux and Kalaydjian* [1990], *Fischer et al.* [2006], *Babadagli and Hatiboglu* [2007] was a Berea sandstone, the materials reported in the work of *Hamon and Vidal* [1986] were performed on a synthetic porous material, and *Zhou et al.* [2002] used a diatomite rock was used. For all the experiments, the wetting-phase was water. For all experiments reported for the first five groups of samples, the nonwetting phase was oil; for the ones reported in the work of *Babadagli and Hatiboglu* [2007] the nonwetting phase was air.

Here, f is the fractional flow function without the influence of capillary pressure, and $D(S_w)$ can be thought of as a capillary dispersion coefficient of the fluid phases.

[15] In countercurrent SI, the two phases flow into opposite directions, i.e., $q_w = -q_{nw}$ (Figure 1), which reduces equation (3) to the nonlinear dispersion equation

$$\phi \frac{\partial S_w}{\partial t} = \frac{\partial}{\partial x} \left[D(S_w) \frac{\partial S_w}{\partial x} \right]. \quad (7)$$

In the following we will only investigate countercurrent SI, and for simplicity denote it as SI. Solutions to equations of the dispersion type show self-similar behavior according to $S_w \propto x\sqrt{t}$, i.e., S_w can be written in terms of the self-similar

variable $\lambda = xt^{-1/2}$ as $S_w = S_w(\lambda)$ [*McWhorter and Sunada*, 1990]. There has been a considerable debate in the literature (for recent reviews see, e.g., *Alava et al.* [2004], *Cai and Yu* [2011], *Hall* [2007]) as to when the \sqrt{t} scaling first proposed by *Lucas* [1918] and *Washburn* [1921] for describing countercurrent imbibition holds. Published experimental data strongly suggests that deviations from this scaling in time only occur for cases where either the porous medium was not rigid (e.g., imbibition into paper, textiles, or rock samples with clay inclusions) [*Alava et al.*, 2004; *Cai and Yu*, 2011; *Hall*, 2007], or gravity and evaporation played a role, which leads to pinning of the wetting fronts (e.g., [*Alava et al.*, 2004; *Delker et al.*, 1996; *Dubé et al.*, 2001]). Thus, assuming a \sqrt{t} scaling is reasonable.

[16] Closely related to this, is the assumption made in equations (1)–(7), where we assumed that k_{rw} , k_{ro} and p_c are unique functions of saturation. Since history effects only occur during a whole imbibition-drainage cycle [Valvatne and Blunt, 2004; Bear, 1972], this assumption is justified. Even for the case without hysteresis, however, several authors (for recent overviews see e.g., [Goel and O'Carroll, 2011; Bottero et al., 2011; Manthey et al., 2008]) proposed that the relation $p_c(S_w) = p_{nw} - p_w$ is not sufficient, and should additionally take the rate of change in saturation $\partial S_w / \partial t$ into account. Allowing for this additional dependence leads to a pseudoparabolic partial differential equation instead of equation (7) whose solutions would also deviate from the \sqrt{t} dependence [Spayd and Shearer, 2011; Hulshof and King, 1998] the more important dynamic effects become. As we will discuss in section 3.3, our results strongly indicate that the inclusion of dynamic capillary effects for SI at the core scale is unnecessary.

2.2. Exact Analytical Solution for SI and the Definition of a Universal Scaling Group

[17] If an analytical solution to equation (7) is known, a general scaling group can immediately be derived from these analytical expressions (Figure 1). In section 2.2 we therefore shortly review known analytical solutions for capillary dominated two-phase flow, and describe an exact analytical solution to equation (7) together with (5). The exact solution is solely based on the assumptions made in section 2.1. It can be viewed [Schmid et al., 2011] as the capillary analog to the Buckley-Leverett solution for viscous dominated flow [Buckley and Leverett, 1942].

[18] While an analytical solution to equation (3) for unidirectional, viscous dominated flow has long been known [Buckley and Leverett, 1942], the counterpart for capillary-dominated flow, equation (7), has been missing, and the derivation of solutions for capillary dominated two-phase flow stayed to be the matter of ongoing intensive research over the last decades (Table 2). The various solutions obtained in the last decade fall into two categories: In the first category, additional assumptions on equation (7) are made, for example a specific functional forms of $D(S_w)$ (Table 2). In the second category [McWhorter and Sunada, 1990], no additional assumptions on the physics or $D(S_w)$ are made. Instead, an additional boundary condition is imposed that specifies the inflow as $q_w(x=0, t) = At^{-1/2}$ where A is a parameter that cannot be chosen freely, but depends on the characteristics of the fluid-rock system according to [McWhorter and Sunada, 1990]

$$A^2 = \frac{\phi}{2} \int_{S_0}^{S_{bc}} \frac{(S_w - S_0)D(S_w)}{F(S_w)} dS_w, \quad (8)$$

and is related to the cumulative water imbibed (Figure 1) by

$$Q_w(t) = \int_0^t q_w(0, t) dt = 2At^{1/2}. \quad (9)$$

$F(S_w)$ is the fractional flow function for countercurrent SI, i.e., it can be viewed as the capillary counterpart to $f(S_w)$ employed in the Buckley-Leverett solution [Buckley

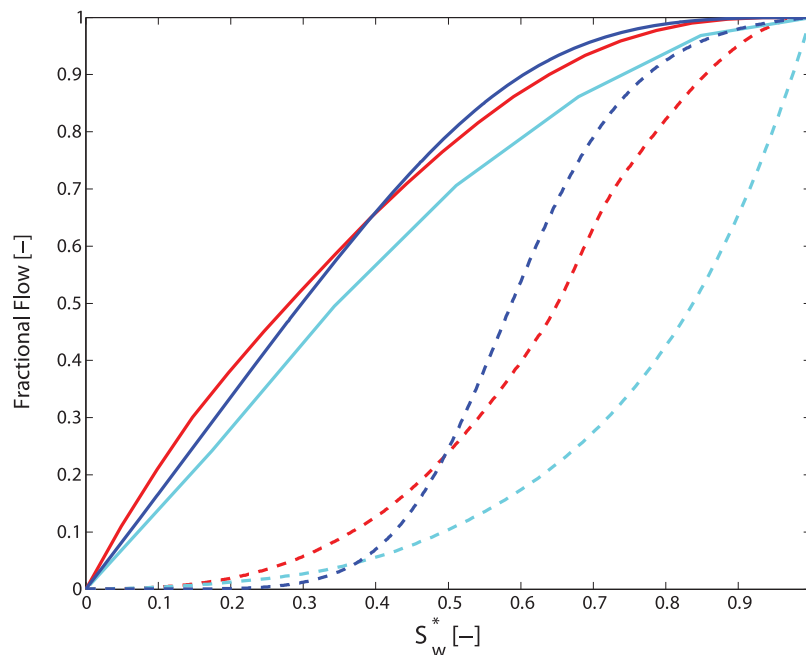


Figure 3. Fractional flow functions f (---) without capillarity and its capillary counterpart F (—) versus saturation. The three cases are for pore-scale predicted [Valvatne and Blunt, 2004] capillary pressure and relative permeability functions for Berea sandstone and a synthetic porous material (blue) and parameter set AA01, a history match that assumes a Darcy model for sandstone (cyan) [Bourbiaux and Kalaydjian, 1990] and parameter set GVB-3, and a non-Darcy-model [Schembre and Kovscek, 2006] for diatomite (red) and parameter set Z-2. The parameter sets are listed in Table 3, and the capillary pressure and relative permeability functions are shown in Figure 2.

and Leverett, 1942] (Figure 3), and is given by the nonlinear equation

$$F(S_w) = 1 - \left[\int_{S_w}^{S_{bc}} \frac{(\beta - S_w)D(\beta)}{F(\beta)} d\beta \right] \left[\int_{S_0}^{S_{bc}} \frac{(\beta - S_0)D(\beta)}{F(\beta)} d\beta \right]^{-1}. \quad (10)$$

Together with A and its derivative F' , the analytical solution for equation (7) with (5) and the condition on $q_w(0, t)$ can then be written as [McWhorter and Sunada, 1990]

$$x(S_w, t) = \frac{2A}{\phi} F'(S_w) t^{1/2} = \frac{Q_w(t)}{\phi} F'(S_w). \quad (11)$$

The inflow condition $q_w(0, t) = At^{-1/2}$ is the one McWhorter and Sunada [1990] and subsequent authors worked with, so that at first the solution (11) seems like just another specific one. However, it can easily be shown [Schmid et al., 2011] that $A = -D(S_0) \frac{dS_w}{d\lambda} |_{\lambda=0}$. Thus, A is exactly such that $q_w(0, t) = -D(S_0) \frac{\partial S_w}{\partial x} |_{x=0}$. This follows from equation (4)

$$\begin{aligned} q_w(x=0, t) &= -D(S_0) \frac{\partial S_w}{\partial x} = -D(S_0) \frac{dS_w}{d\lambda} |_{\lambda=0} \frac{\partial \lambda}{\partial x} \\ &= -D(S_0) \frac{dS_w}{d\lambda} |_{\lambda=0} t^{-1/2} = At^{-1/2}. \end{aligned} \quad (12)$$

Consequently, A does not describe forced imbibition, but rather is such that the inflow $q_w(0, t)$ occurs spontaneously into the porous medium because of the saturation gradients at the boundary and the resulting gradients in capillary pressure only. Thus, the boundary condition on $q_w(0, t)$ is redundant, and equation (11) describes the standard situation found in the laboratory. Any further derivations of analytical solutions (Table 2) for the countercurrent case seem unnecessary [Schmid et al., 2011].

[19] Equation (11) can be used to introduce a scaling group that incorporates all the information present in the two-phase Darcy equation. To derive a scaling group from equation (11), we first normalize x by the characteristic length L_c through x/L_c where [Ma et al., 1997]

$$L_c = \sqrt{\frac{V_b}{\sum_{i=1}^n A_i/l_{A_i}}}. \quad (13)$$

V_b is the bulk volume of the matrix, A_i the area open to imbibition with respect to the i th direction, and l_{A_i} is the distance that the imbibition front travels from the imbibition face to the no-flow boundary. L_c thus compensates for different experimental boundary conditions, i.e., for which sides of a rock sample are sealed in the experiment, and which are open to flow. L_c also has the physical interpretation of quantifying the length a wetting front can travel without meeting a boundary or another imbibition front [Ma et al., 1997]. While the question of how to incorporate the influence of viscosity ratios, wettability information,

and so forth into scaling groups remains open, the correct incorporation of different experimental boundary conditions with the help of L_c has been confirmed [Ma et al., 1997; Zhang et al., 1996].

[20] Although the solutions have been derived for an infinite medium according to the initial condition (5), the x profile for any time $0 \leq t < \infty$ has a finite extend (Figure 1). Thus, the solution is valid in a finite matrix block as long as the wetting front has not reached the end of the block and has not interfered with other wetting fronts invading from other areas A_i . The time t^* when the solutions stop to be valid in a finite matrix block of characteristic length L_c can hence be obtained from setting $x(S_{wi}, t^*) = L_c$ which yields

$$t^* = \left[\frac{L_c \phi}{2AF'(S_i)} \right]^2. \quad (14)$$

For any $0 < t < t^*$ the profiles are given by (11), and Q_w is given by (9). In Figure 4 we show the analytical solution for Q_w versus the dimensionless time defined below for the data set where the sample-specific capillary-hydraulic properties are known (violet squares in Figure 4, data set GVB-3 in Table 3). For early times, the analytical prediction is in good agreement with the data, but for late times it fails to predict the slow down in recovery. This is because for $t > t^*$, the end of the block or another wetting front influences the saturation profile, and equations (11) and (9) are no longer valid.

[21] We now use that $Q_w(t)$ can be calculated explicitly by equation (9), and define a scaling group based on the cumulative wetting phase imbibed at any given t and the normalized pore volume in 1-D, $\phi \cdot L_c$ (Figure 1)

$$t_d = \left[\frac{Q_w(t)}{\phi L_c} \right]^2 = \left[\frac{2A}{\phi L_c} \right]^2 t = \tau_c t. \quad (15)$$

Thus, t_d rigorously incorporates all the parameters present in the two-phase Darcy formulation, and τ_c can be thought of as a characteristic time that quantifies both the influence of the capillary-hydraulic properties and the physical dimensions. We note, that this approach is fundamentally different from dimensionless groups that try to predict parameters like S_{or} from dimensionless groups [e.g., Anton and Hilfer, 1999]. We next show the validity of t_d by correlating 42 published experiments, and comparing t_d to the often used group by Ma et al. [1997]. Also, t_d can be used as a theoretical tool to assess the validity of a conventional Darcy description of SI. The good correlation obtained in Figure 4 shows that t_d is the general scaling group for SI, and forms the so far missing center piece for upscaling, modeling and simulating diverse systems, where SI plays a role. We then show how t_d is central for two key applications, namely, fracture flow modeling and imbibition-germination modeling in plant seeds.

3. Results

3.1. Validity of the Universal Scaling Group

[22] To demonstrate the validity of the proposed scaling group equation (15), we correlated the results of 42 published SI experiments with t_d (Figure 4). In the experiments the recovery R of the nonwetting phase was measured over

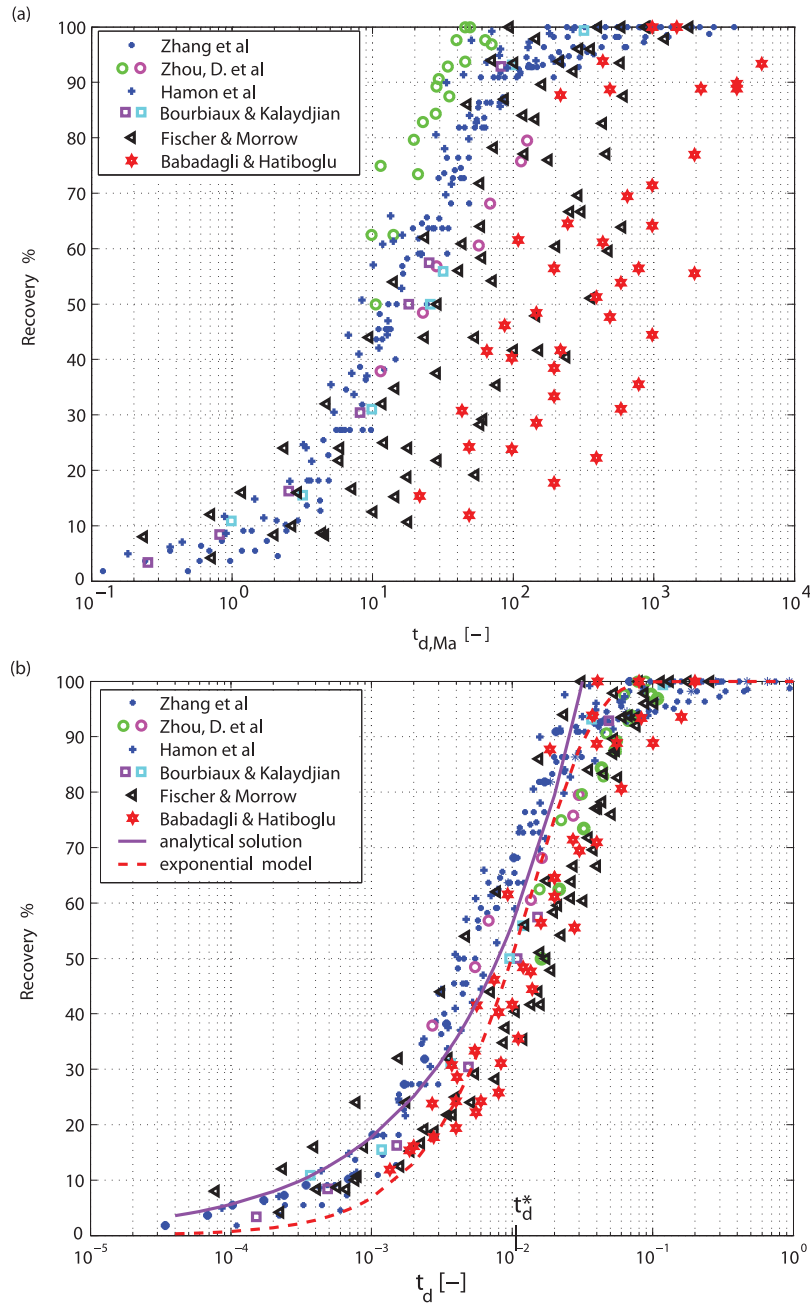


Figure 4. Recovery of the displaced fluid phase versus time. (a) Time is scaled according to the scaling group proposed by [Ma et al., 1997] (Table 1). But the scaling does not result in the collapse of the data onto a single curve. The scaling group can only give a good correlation if the proportionality constant c (Table 1) is similar for the different data sets which is not the case here. (b) Scaling of the experimental data with our proposed nondimensional time $t_d = \left[\frac{Q_w(t)}{\phi \cdot L_c} \right]^2$. The data falls onto a curve with little scatter, independent of the material and/or fluid characteristics. This indicates that the Darcy model is suitable for characterizing SI. The analytical solution is valid as long as the dimensionless time satisfies $t_d \leq t_d^* = \tau_c t^*$. To correlate the behavior for the whole time range, an exponential model [Aronofsky et al., 1958] is used.

time, and we correlated the physical time with t_d . The experimental data sets were chosen such that the three central open aspects of scaling groups—a wide range of viscosity ratios with the special case of μ_n tending toward zero, the presence of an initial wetting phase, and different capillary-hydraulic properties—are covered. The experiments were

performed on three different porous materials, a synthetic porous medium, Berea sandstone, and diatomite (Figure 2), a wide range of nonwetting phase to wetting phase viscosity ratios ($0.008 \leq \mu_{nw}/\mu_w \leq 64$), initial water content ($0\% \leq S_0 \leq 40\%$), characteristic length-scales ($0.54 \text{ cm} \leq L_c \leq 40 \text{ cm}$), and water potential ($18\% \leq 1 - S_0 - S_{nr}$

$\leq 70\%$, where S_{nr} is the residual saturation of the nonwetting phase). The wetting phase was water and the nonwetting phase oil or air. Table 3 lists all experimental conditions.

[23] We note that while the experiments considered here are for different capillary-hydraulic properties, they all show strongly water-wet behavior, i.e., $p_c > 0$ over the whole saturation range (Figure 2). The analytical solution given in equation (11) has been derived for boundary conditions, that are not suitable for treating mixed-wet systems, i.e., for systems where $p_c < 0$ for some $S_w < 1 - S_{nr}$ [Morrow and Mason, 2001]. How to modify the analytical solution, equation (2), for the mixed-wet case is currently investigated.

[24] For comparison, we also correlated the data with one of the most commonly used scaling groups (Figure 4); the improvement is significant and immediately apparent. Equation (15) reduces the maximal horizontal scatter (i.e., the one for a fixed recovery rate) from a factor of greater than 100 down to approximately 5, and the maximal vertical scatter (i.e., the one for a fixed t_d) from approximately 0.8 to 0.3. This is a remarkably good result given the widely different experimental conditions and thus experimental noise.

[25] To further improve the scaling, one should use the capillary-hydraulic properties for the specific sample when calculating t_d . Most data sets available in the literature only report SI measurements or (k_{rw}, k_{rn}) relationships, or p_c curves. In order to calculate t_d we therefore assumed that the (k_{rw}, k_{rn}, p_c) sets measured for a certain rock type are representative for a given material, see section 3.3. It is also interesting to note, that the data in Figure 4 scatters around the curve given by the analytical solution that has been calculated for data where the sample-specific capillary-hydraulic properties are known. It is not clear, whether this is true only for particular data sets, or shows that the analytical solution is a master curve for early times on which all data would collapse if better predictions for the capillary-hydraulic properties were known. One would have to calculate the analytical prediction for more data sets where the sample specific properties are known. As we explained, however, complete data sets are rare.

3.2. Prediction of the Validity of Specialized Groups

[26] The Lucas-Washburn correlation together with some of the previously defined scaling groups are listed in Table 1. Previous scaling groups are related to our scaling group through a proportionality factor c . Since our group is the general one, explicit expressions for c can be derived. It is now apparent that previous authors (unknowingly) derived successively better approximations to the integral in equation (8), making the proportionality constant c increasingly simple. Many of the previously derived t_d can be obtained from simple back-of-the-envelope calculations as special cases of equation (15).

[27] Equation (15) can also be used to derive new scaling groups that are tailored for a specific SI system by using an approximation for A that is appropriate for that specific case. The ability of such a special t_d to correlate a set of experiments depends on the similarity of c for the individual data sets, and thus allows for a rigorous prediction of their validity and a judgment as to which parameters are negligible. This property can be used to derive the validity

of some of the phenomenologically derived groups like that of [Ma *et al.*, 1997] (Table 1, Figure 4). The scaling group in Figure 4 can only give a good correlation if the proportionality constant c (Table 1) is similar for the different data sets. This is the case for some of the SI experiments on sandstone (blue asterisk in Figure 4) and the synthetic material (blue plus in Figure 4) from which Ma *et al.* [1997] derived the correlation phenomenologically. Here, the viscosity ratio is approximately one, the initial fluid content is similar and the capillary hydraulic properties were the same. These conditions result in similar functional form of F , similar integral boundaries, and the same integrand for c , respectively. Depending on which assumption is violated, five subgroups different from the (blue asterisk and plus)-curve emerge: The subgroup for (1) different S_0 , different capillary-hydraulic properties (diatomite with (2) high and (3) low μ_{nw}/μ_w), (4) sandstone with strongly varying μ_{nw}/μ_w , and (5) sandstone containing gas, i.e., a nonwetting phase with neglectable μ_{nw} .

3.3. Do We Need Dynamic Effects in p_c to Model Si?

[28] While the main part of this paper is dedicated to derive the first scaling group that rigorously includes all the information given in the standard Darcy formulation, the validity of t_d for such a wide range of data sets also has theoretical implications: It strongly indicates that a functional relationship for p_c which additionally includes dynamic effects is not necessary for describing SI at the core scale.

[29] In the foregoing analysis, it was assumed that p_c is a unique function of S_w only. Recently, the dependence of p_c on S_w only has been questioned by several authors (for recent overviews see, e.g., Goel and O'Carroll [2011], Bottero *et al.* [2011], Manthey *et al.* [2008]), and it has been proposed that an additional dependence on $\tau \cdot \partial S_w / \partial t$ should be included, where τ is a proportionality factor that possibly depends on material characteristics, the fluid saturations, and the length scale. Some authors ([Barenblatt *et al.*, 2003; Le Guen and Kovscek, 2006]; for a recent overview see Hall [2007]) argue that nonequilibrium effects are especially important for the case of countercurrent SI due to the filling process of the pores by the wetting fluid. Several models have been proposed to incorporate this dynamic effect. For example Hassanizadeh and Gray [1990] and Kalaydjian [1992] consider the linearized form

$$p_o - p_w - p_c = \tau(S_w) \cdot \frac{\partial S_w}{\partial t}. \quad (16)$$

Obviously, τ determines the importance of the dynamic effects, and while it is known that τ can vary over several orders of magnitude [Manthey *et al.*, 2008], the functional dependence of τ , and when/if dynamic effects have to be considered, remains unclear. Thus, recent work has tried to shed light on the exact dependence of τ , to resolve the in part conflicting results for different models, and provide the often missing experimental confirmation for the theoretical considerations [Goel and O'Carroll, 2011]. In this context, the scaling group t_d can be used to measure the validity of the standard formulation for p_c for describing SI. If dynamic effects are not negligible, this has two consequences for the scaling with t_d .

[30] First, the incorporation of the saturation change makes equation (7) pseudoparabolic whose solutions would

deviate from the \sqrt{t} dependence [Spayd and Shearer, 2011; Hulshof and King, 1998] the more important dynamic effects become. Consequently, the \sqrt{t} given through t_d as such should fail. As we have outlined in section 2.1, the experimental evidence for a \sqrt{t} scaling—as long as the assumptions of a rigid, homogeneous porous medium, negligible gravity, and no evaporation are valid—is overwhelming. What is more important, however, is the fact that the data sets we chose vary all the key parameters. If dynamic effects played any role, one would expect that at least one data set significantly diverges from the \sqrt{t} scaling. We do not observe this.

[31] Second, if τ really depends on material properties as has been suggested, then the wide parameter variation of the data sets we use should also lead to a wider horizontal spread in Figure 4. As the scaling with $t_{d, Ma}$ has shown, failing to account for relevant parameters results in the emergence of different subgroups for the different data sets. While the maximal horizontal scatter for t_d (Figure 4) is still around 5, the reported values for τ vary several orders of magnitude [Manthey et al., 2008]. Thus, if dynamic effects matter for SI at the core scale, one should obtain a significantly worse horizontal spread. We also note here, that although we speak of length scales typical for the core scale, we chose data sets where L_c varies by almost an order of magnitude (Table 3). Thus, if τ depended on the length scales as has been suggested [Bottero et al., 2011], this also should result in a wider horizontal spread.

[32] To rigorously test the second part, the method used for calculating the capillary-hydraulic properties in A must not presume the validity of the standard Darcy equation. It is common practice [Gummerson et al., 1979], to obtain k_{rw} , k_{rn} , and p_c from solving an inverse problem that assumes the validity of the standard Darcy equation. Obviously, if all the capillary-hydraulic relationships in the sample data set were obtained this way, then t_d defined in equation (2) would give an excellent correlation, since it is based on an exact solution of Darcy's equation, and the constitutive relations would have been determined to fit the data set, possibly hiding the missing of τ . The question whether the standard Darcy model without dynamic p_c relations model is applicable for capillary flow would thus be bypassed. For the experiments performed on Berea sandstone and the synthetic porous medium, we therefore use pore-scale predictions of the relative permeabilities and the capillary pressure [Valvatne and Blunt, 2004] (Figure 2), rather than modeling (k_{rw} , k_{rn} , p_c) through inverse simulation of experimental data.

[33] For the synthetic material, only k_{rw} and k_{rn} have been measured. However, the curves closely resemble that for the sandstone, which indicates that the two materials have a similar pore structure. Therefore the pore-scale predictions made for the sandstone sample were used. For the water-air experiments on sandstone, the measured and pore-scale predicted k_{rw} and k_{rn} were similar to that of the water-oil system [Valvatne and Blunt, 2004]. Hence, we used the same (k_{rw} , k_{rn} , p_c) set as for the water-oil system. To account for effects of K and surface tensions σ , we used a Leverett J scaling [Bear, 1972]

$$p_c = \sigma \sqrt{\frac{\phi}{K}} J(S_w^*), \quad (17)$$

where $S_w^* = (S_w - S_{wr}) / (1 - S_{or} - S_{wr})$ is the normalized saturation, and S_{wr} is the residual water phase. We note again, that we used the same (k_{rw} , k_{rn} , J) set for a certain material, rather than direct measurements for the specific sample. To further reduce the scatter, sample specific relations should be used. For comparison with the pore-scale predicted relations, the capillary-hydraulic properties obtained from a standard Darcy and a history match that includes a dynamic p_c were used for some of the sandstone experiments and the diatomite experiments, respectively. For the general scaling t_{db} , the data sets collapse onto a curve with little scatter (Figure 4) showing that the behavior is well characterized by t_d . Since t_d contains all the information present in the Darcy model, and its validity has not been assumed to calculate the capillary-hydraulic properties in A , this strongly indicates that the Darcy model is suitable for characterizing and modeling SI at the core scale. It is important to point out, that for viscous or gravity dominated flow the rate of change in saturation would be higher, and therefore the influence of nonequilibrium effects might not be negligible any more.

3.4. Applications of the Universal Scaling Group

[34] In addition to the theoretical insight t_d yields as to whether Darcy's model is applicable, in an SI application it is often desirable to describe the influence of certain parameters under certain conditions to optimize the system. If the assumptions for Darcy's equation hold, our scaling group provides a simple, yet rigorous, starting point for optimizing the modeling of any SI system, and strongly reduces the need for lengthy SI laboratory experiments. We give two very different examples, one from modeling fracture flow, the other one from plant science.

[35] Our first application are dual-porosity models where scaling groups build the center piece. Dual-porosity models describe the fluid exchange between a high-permeability or mobile region and a low-permeability, immobile region. The models are often used as field-scale representations of fractured reservoirs and aquifers, by separating the subsurface model into stagnant, low-permeability regions (the rock matrix blocks) and high-permeability regions (the fracture network). A general form for the fluid transfer T between the fracture matrix—or more generally mobile-immobile—regions that fully accounts for heterogeneities in wettabilities and phase mobilities has been a long-standing question [Barenblatt et al., 1960; Warren and Root, 1963]. To predict the shape of the correlated data over the whole time range, the analytical solutions for $x(S_w, t)$ and $Q_w(t)$ presented in section 2.2 cannot be used since they are only valid as long as $t < t^*$. Thus, instead of predicting the s shape of the correlated data (Figure 4), they instead would predict that Q_w increases indefinitely. Therefore, to fit the data we instead use an exponential model $R = 1 - e^{-\alpha t_d}$ [Aronofsky et al., 1958] with $\alpha \approx 70$. Since the transfer T between fracture and matrix satisfies $T = \phi \frac{dR}{dt}$, it follows that $T(R) = \alpha \phi \tau_c (1 - R)$. Furthermore, as A contains all the information about the capillary-hydraulic properties and the initial fluid content, but is independent of L_c , it shows the influence of the porous structure and fluid characteristics on SI. For sandstone with water as the wetting phase and oil as the nonwetting phase ($\mu_n/\mu_w = 39$, $S_{wi} = 0$), we found $A \approx 7 \times 10^{-6} m/\sqrt{s}$, while for diatomite (with $\mu_n/\mu_w = 25$, $S_{wi} = 0$) we found

$A \approx 1.5 \times 10^{-5} m/\sqrt{s}$, i.e., the fluxes $Q_w(t)$ differ by an order of magnitude. This shows that geological heterogeneity present in the subsurface can give rise to widely different time scales, independent of different length scales or fluid viscosities. The coefficient A can be used to rigorously capture this behavior through a multirate model [Di Donato et al., 2007; Haggerty and Gorelick, 1995].

[36] The second example considers imbibition damage during water uptake in porous plant seeds. The transient behavior of the SI process is crucial for the field emergence of commercial seeds, and determining favorable conditions for SI with the help of coupled imbibition-germination models is of great practical interest [Finch-Savage et al., 2005]. In imbibition-germination models, the water content in a seed is estimated from an imbibition model. The so-obtained value for the water content is then used to calculate the germination time, i.e., the time until the seed starts growing. For these models, the product $\beta = \alpha\phi\tau_c$ is an explicit expression for the proportionality constant used in coupled imbibition-germination models [Finch-Savage et al., 2005]. Contrary to the phenomenologically derived constant however, β can be used for example to predict how the seed-imbibition depends on L_c and thus on seed size without the need to perform the lengthy and difficult laboratory experiments on plant seeds that up to now have been necessary.

4. Conclusions and Outlook

[37] Capturing the influence of key parameters in SI through scaling groups is central for many applications, and the question how to formulate a general group has been open for over 90 years. We derived the first universal scaling group for SI for water-wet rocks that incorporates all the information present in the two-phase Darcy model. Our scaling group was derived rigorously from an exact solution to Darcy's equation for spontaneous imbibition (Table 2), without the introduction of any fitting parameters by relating the cumulative water phase imbibed to the normalized pore volume. The new scaling group is a "master equation" for scaling groups, and contains many of the previously derived scaling groups as special cases (Table 1). We demonstrated how the generality of our approach allows the prediction of the validity range of specialized groups. We showed the validity of our scaling group by correlating 42 published imbibition studies for water-wet rocks and different materials, a wide range of viscosity ratios, initial water content and characteristic length scales (Table 3). The correlated data falls onto one curve (Figure 1). This strongly indicates that the standard Darcy model is suitable for describing SI, contrary to what recently has been hypothesized. To further improve the scaling, we suggest that the capillary-hydraulic properties for the specific sample for calculating t_d should be used, rather than using one set for any sample of a given rock type. For early times, the data in Figure 4 scatters around the curve given by the analytical solution. It is not clear whether this is true only for particular data sets, or shows that the analytical solution is a master curve all data would collapse on for early times if better predictions for the capillary-hydraulic properties were available. This should be further investigated with data sets where the measurements and the sample specific properties are available. Our results are applicable to any situation

where SI plays a role and where gravity can be ignored. We provided two key examples where our results can be used. First, we demonstrated how based on t_d the first fluid transfer function can be obtained that rigorously captures all the capillary-hydraulic properties in dual-porosity models for fracture flow, and we showed how the constant A is a measure for the subsurface heterogeneity that exists due to differences in pore structure. As a second example, we showed how germination models for plant seeds can easily account for seed size and other key parameters, thus eliminating the necessity of lengthy laboratory experiments.

[38] **Acknowledgments.** We thank the following for the financial support for this work: The CMG Reservoir Simulation Foundation, the ExxonMobil Research Alliance "Fundamental Controls of Flow in Carbonates" (FC)², and the Edinburgh Collaborative of Subsurface Science and Engineering, a joint research institute of the Edinburgh Research Partnership in Engineering and Mathematics. The authors cordially thank M. J. Blunt, P. D'Odorico, E. S. Woollen, T. Driesner, O. J. Hehmeyer and K. S. Sorbie for discussions. The constructive comments of the anonymous reviewers are gratefully acknowledged.

References

- Alava, M., M. Dubé, and M. Rost (2004), Imbibition in disordered media, *Adv. Phys.*, 53(2), 83–175.
- Anderson, R., B. Tohidi, and J. B. W. Webber (2009), Gas hydrate growth and dissociation in narrow pore networks: Capillary inhibition and hysteresis phenomena, *Geol. Soc. London Spec. Publ.*, 319(1), 145–159.
- Anton, L., and R. Hilfer (1999), Trapping and mobilization of residual fluid during capillary desaturation in porous media, *Phys. Rev. E*, 59(6), 6819–6823.
- Aronofsky, J. S., L. Masse, and S. G. Natanson (1958), A model for the mechanism of oil recovery from the porous matrix due to water invasion in fractured reservoirs, *Petrol. Trans. AIME*, 213, 17–19.
- Babadagli, T., and C. U. Hatiboglu (2007), Analysis of counter-current gas-water capillary imbibition transfer at different temperatures, *J. Petrol. Sci. Eng.*, 55(3–4), 277–293.
- Barenblatt, G. I., I. P. Zheltov, and I. N. Kochina (1960), Basic concepts in the theory of seepage of homogeneous liquids in fissured rocks, *J. Appl. Math. Mech.*, 24(5), 1286–1303.
- Barenblatt, G. I., V. M. Entov, and V. M. Ryzhik (1990), *Theory of Fluid Flows Through Natural Rocks*, Springer, New York.
- Barenblatt, G. I., T. W. Patzek, and D. B. Silin (2003), The mathematical model of nonequilibrium effects in water-oil displacement, *SPE J.*, 8(4), 409–416.
- Bear, J. (1972), *Dynamics of Fluids in Porous Media*, Dover, New York.
- Bickle, M. J. (2009), Geological carbon storage, *Nat. Geosci.*, 2(12), 815–818.
- Bottero, S., S. M. Hassanizadeh, P. J. Kleingeld, and T. J. Heimovaara (2011), Nonequilibrium capillarity effects in two-phase flow through porous media at different scales, *Water Resour. Res.*, 47, W10505, doi:10.1029/2011WR010887.
- Bourbiaux, B., and F. Kalaydjian (1990), Experimental study of cocurrent and countercurrent flows in natural porous media, *SPE Res. Eng.*, 5(3), 361–368.
- Brusseau, M. L. (1992), Rate-limited mass transfer and transport of organic solutes in porous media that contain immobile immiscible organic liquid, *Water Resour. Res.*, 28(1), 33–45, doi:10.1029/91WR02498.
- Buckley, S. E., and M. C. Leverett (1942), Mechanisms of fluid displacement in sands, *Trans. AIME*, 146, 107116.
- Cai, J., and B. Yu (2011), A discussion of the effect of tortuosity on the capillary imbibition in porous media, *Transp. Porous Media*, 89, 1–13, doi:10.1007/s11242-011-9767-0.
- Chaturvedi, T., J. M. Schembre, and A. R. Kovscek (2009), Spontaneous imbibition and wettability characteristics of powder river basin coal, *Int. J. Coal Geol.*, 77(1–2), 34–42.
- Chen, J., M. A. Miller, and K. Sepehrnoori (1995), Theoretical investigation of countercurrent imbibition in fractured reservoir matrix blocks, *Pap. 29141-MS, SPE Reservoir Simul. Symp.*, 12–15 Feb., Society of Petroleum Engineers, San Antonio, Tex.
- Chen, Z. X. (1988), Some invariant solutions to two-phase fluid displacement problems including capillary effect, *SPE Res. Eng.*, 3(2), 69–700.

- Cil, M., and J. C. Reis (1996), A multi-dimensional, analytical model for counter-current water imbibition into gas-saturated matrix blocks, *J. Petrol. Sci. Eng.*, 16(1–3), 61–69.
- Civan, F., and M. Rasmussen (2001), Asymptotic analytical solutions for imbibition waterfloods in fractured reservoirs, *SPE J.*, 6(2), 171–181.
- Clennell, M. B., M. Hovland, J. S. Booth, P. Henry, and W. J. Winters (1999), Formation of natural gas hydrates in marine sediments 1. Conceptual model of gas hydrate growth conditioned by host sediment properties, *J. Geophys. Res.*, 104(B10), 22,985–23,003.
- Delker, T., D. B. Pengra, and P. Wong (1996), Interface pinning and the dynamics of capillary rise in porous media, *Phys. Rev. Lett.*, 76(16), 2902–2905.
- Di Donato, G., and M. J. Blunt (2004), Streamline-based dual-porosity simulation of reactive transport and flow in fractured reservoirs, *Water Resour. Res.*, 40, W04203, doi:10.1029/2003WR002772.
- Di Donato, G., H. Lu, Z. Tavassoli, and M. Blunt (2007), Multirate-transfer dual-porosity modeling of gravity drainage and imbibition, *SPE J.*, 12(1), 77–88.
- Dubé, M., S. Majaniemi, M. Rost, M. J. Alava, K. R. Elder, and T. Ala-Nissila (2001), Interface pinning in spontaneous imbibition, *Phys. Rev. E*, 64(5), 051605.
- Finch-Savage, W. E., H. R. Rowse, and K. C. Dent (2005), Development of combined imbibition and hydrothermal threshold models to simulate maize (*Zea mays*) and chickpea (*Cicer arietinum*) seed germination in variable environments, *New Phytol.*, 165(3), 825–838.
- Fischer, H., S. Wo, and N. Morrow (2006), Modeling the effect of viscosity ratio on spontaneous imbibition, *SPE Reservoir Eval. Eng.*, 102641, 577–589.
- Fokas, A. S., and Y. C. Yortsos (1982), On the exactly solvable equation $s_t = [(\beta s + \gamma)^{-2} s_{,xx} + \alpha(\beta s + \gamma)^{-2} s_x]$ occurring in two-phase flow in porous media, *SIAM J. Appl. Math.*, 42(2), 318–332, doi:10.1137/0142025.
- Goel, G., and D. M. O'Carroll (2011), Experimental investigation of nonequilibrium capillarity effects: Fluid viscosity effects, *Water Resour. Res.*, 47(9), W09507, doi:10.1029/2010WR009861.
- Gummerson, R. J., C. Hall, W. D. Hoff, R. Hawkes, G. N. Holland, and W. S. Moore (1979), Unsaturated water flow within porous materials observed by NMR imaging, *Nature*, 281, 56–57.
- Haggerty, R., and S. M. Gorelick (1995), Multiple-rate mass transfer for modeling diffusion and surface reactions in media with pore-scale heterogeneity, *Water Resour. Res.*, 31(10), 2383–2400.
- Hall, C. (2007), Anomalous diffusion in unsaturated flow: Fact or fiction?, *Cem. Concr. Res.*, 37(3), 378–385.
- Hamon, G., and J. Vidal (1986), Scaling-up the capillary imbibition process from laboratory experiments on homogeneous and heterogeneous samples, *SPE 15852, Proceedings of the European Petroleum Conference*, 20–22 Oct., pp. 37–49, Society of Petroleum Engineers, London.
- Handy, L. L. (1960), Determination of effective capillary pressures for porous media from imbibition data, *Petrol. Trans. AIME*, 219, 75–80.
- Hassanizadeh, S. M., and W. G. Gray (1990), Mechanics and thermodynamics of multiphase flow in porous media including interphase boundaries, *Adv. Water Res.*, 13(4), 169–186.
- Hulshof, J., and J. R. King (1998), Analysis of a darcy flow model with a dynamic pressure saturation relation, *SIAM J. Appl. Math.*, 59, 318–346.
- Jadhunandan, P. P., and N. R. Morrow (1991), Spontaneous imbibition of water by crude oil/brine/rock systems, *In Situ*, 15(4), 319–345.
- Juanes, R., E. J. Spiteri, F. M. Orr Jr., and M. J. Blunt (2006), Impact of relative permeability hysteresis on geological CO₂ storage *Water Resour. Res.*, 42, W12418, doi:10.1029/2005WR004806.
- Kalaydjian, F. J. M. (1992), Dynamic capillary pressure curve for water/oil displacement in porous media: Theory vs. experiment, paper 24813, *SPE Annu. Tech. Conf. and Exhibition*, pp. 491–506, SPE, Allen, Tex.
- Kashchiev, D., and A. Firoozabadi (2002), Analytical solutions for 1-D counter-current imbibition in water-wet media, *SPE J.*, 8(4), 401–408.
- Le Guen, S. S., and A. R. Kovscek (2006), Nonequilibrium effects during spontaneous imbibition, *Transp. Porous Media*, 63(1), 127–146.
- Li, K., and R. Horne (2006), Generalized scaling approach for spontaneous imbibition: an analytical model, *SPE Reservoir Eval. Eng.*, 9(3), 251–258.
- Li, K., and R. N. Horne (2009), Method to evaluate the potential of water injection in naturally fractured reservoirs, *Transp. Porous Media*, 83, 699–709.
- Li, Y., N. R. Morrow, and D. Ruth (2003), Similarity solution for linear counter-current spontaneous imbibition, *J. Petrol. Sci. Eng.*, 39(3–4), 309–326.
- Lucas, R. (1918), Über das Zeitgesetz des kapillaren Aufstiegs von Flüssigkeiten, *Colloid Polymer Sci.*, 23(1), 15–22.
- Ma, S., N. R. Morrow, and X. Zhang (1997), Generalized scaling of spontaneous imbibition data for strongly water-wet systems, *J. Petrol. Sci. Eng.*, 18(3–4), 165–178.
- Manthey, S., S. M. Hassanizadeh, R. Helmig, and R. Hilfer (2008), Dimensional analysis of two-phase flow including a rate-dependent capillary pressure-saturation relationship, *Adv. Water Res.*, 31(9), 1137–1150.
- Marmur, A. (2003), Kinetics of penetration into uniform porous media: Testing the equivalent-capillary concept, *Langmuir*, 19(14), 5956–5959.
- Mason, G., H. Fischer, N. R. Morrow, and D. W. Ruth (2010), Correlation for the effect of fluid viscosities on counter-current spontaneous imbibition, *J. Petrol. Sci. Eng.*, 72(1–2), 195–205.
- Mattax, C. C., and J. R. Kyte (1962), Imbibition oil recovery from fractured, water-drive reservoir, *SPE J.*, 2(2), 177–184.
- McWhorter, D. B., and D. K. Sunada (1990), Exact integral solutions for two-phase flow, *Water Resour. Res.*, 26(3), 399–413.
- Mirzaei-Paiaman, A., M. Masihi, and D. C. Standnes (2011), An analytic solution for the frontal flow period in 1D counter-current spontaneous imbibition into fractured porous media including gravity and wettability effects, *Transp. Porous Media*, 89, 1–14, doi:10.1007/s11242-011-9751-8.
- Morrow, N. R., and G. Mason (2001), Recovery of oil by spontaneous imbibition, *Curr. Opin. Colloid Interface Sci.*, 6(4), 321–337, doi:10.1016/S1359-0294(01)00100-5.
- Muskat, M. (1949), *Physical Principles of Oil Production*, McGraw Hill, New York.
- Parrish, D. J., and A. C. Leopold (1977), Transient changes during soybean imbibition, *Plant Physiol.*, 59(6), 1111–1115.
- Pentland, C. H., R. El-Maghraby, S. Iglauer, and M. J. Blunt (2011), Measurements of the capillary trapping of super-critical carbon dioxide in Berea sandstone, *Geophys. Res. Lett.*, 38(6), L06401, doi:10.1029/2011GL046683.
- Philip, J. R. (1960), A very general class of exact solutions in concentration-dependent diffusion, *Nature*, 4708, 233.
- Rangel-German, E. R., and A. R. Kovscek (2002), Experimental and analytical study of multidimensional imbibition in fractured porous media, *J. Petrol. Sci. Eng.*, 36(1–2), 45–60.
- Rapoport, L. A. (1955), Scaling laws for use in design and operation of water-oil flow models, *Trans. AIME*, 204, 143–150.
- Rasmussen, M. L., and F. Civan (1998), Analytical solutions for waterfloods in fractured reservoirs obtained by an asymptotic approximation, *SPE J.*, 3(3), 249–252.
- Reis, J. C., and M. Cil (1993), A model for oil expulsion by counter-current water imbibition in rocks: One-dimensional geometry, *J. Petrol. Sci. Eng.*, 10(2), 97–107.
- Ruth, D. W., and J. K. Arthur (2011), A revised analytic solution to the linear displacement problem including capillary pressure effects, *Transp. Porous Media*, 86, 881–894.
- Ruth, D. W., Y. Li, G. Mason, and N. R. Morrow (2007), An approximate analytical solution for counter-current spontaneous imbibition, *Transp. Porous Media*, 66(3), 373–390.
- Sanchez Bujanos, J. L., M. A. Miller, and K. Sephermoori (1998), Scaling parameters for characterizing waterflood recovery from anisotropic matrix blocks in naturally fractured reservoirs, paper 39626, *SPE Int. Petrol. Conf.*, 61–69, Society of Petroleum Engineers, Villahermosa, Mexico.
- Schembre, J. M., and A. R. Kovscek (2006), Estimation of dynamic relative permeability and capillary pressure from counter-current imbibition experiments, *Transp. Porous Media*, 65(1), 31–51.
- Schmid, K. S., S. Geiger, and K. S. Sorbie (2011), Semianalytical solutions for co- and counter-current imbibition and dispersion of solutes in immiscible two-phase flow, *Water Resour. Res.*, 47(2), W02550, doi:10.1029/2010WR009686.
- Spayd, K., and M. Shearer (2011), The Buckley-Leverett equation with dynamic capillary pressure, *SIAM J. Appl. Math.*, 71, 1088–1108.
- Tavassoli, Z., R. W. Zimmerman, and M. J. Blunt (2005a), Analytical analysis for oil recovery during counter-current imbibition in strongly water-wet systems, *Transp. Porous Media*, 58(1), 173–189.
- Tavassoli, Z., R. W. Zimmerman, and M. J. Blunt (2005b), Analysis of counter-current imbibition with gravity in weakly water-wet systems, *J. Petrol. Sci. Eng.*, 48(1–2), 94–104.
- Valvatne, P. H., and M. J. Blunt (2004), Predictive pore-scale modeling of two-phase flow in mixed wet media, *Water Resour. Res.*, 40, W07406, doi:10.1029/2003WR002627.
- Warren, J. E., and P. J. Root (1963), The behavior of naturally fractured reservoirs, *SPE J.*, 3(3), 245–255.
- Washburn, E. W. (1921), The dynamics of capillary flow, *Phys. Rev.*, 17(3), 273–283.

- Wu, Y. S., and L. Pan (2003), Special relative permeability functions with analytical solutions for transient flow into unsaturated rock matrix, *Water Resour. Res.*, 39(4), 1104, doi:10.1029/2002WR001495.
- Yortsos, Y. C., and A. S. Fokas (1983), An analytical solution for linear water-flood including the effects of capillary pressure, *SPE J.*, 23(1), 115–124.
- Zhang, X., N. Morrow, and S. Ma (1996), Experimental verification of a modified scaling group for spontaneous imbibition, *SPE Res. Eng.*, 11(4), 280–285.
- Zhou, D., L. Jia, J. Kamath, and A. R. Kovscek (2002), Scaling of counter-current imbibition processes in low-permeability porous media, *J. Petrol. Sci. Eng.*, 33(1–3), 61–74.
- Zimmerman, R. W., and G. S. Bodvarsson (1989), An approximate solution for one-dimensional absorption in unsaturated porous media, *Water Resour. Res.*, 25(6), 1422–1428.
- Zimmerman, R. W., and G. S. Bodvarsson (1991), A simple approximate solution for horizontal infiltration in a brooks-corey medium, *Transp. Porous Media*, 6(2), 195–205.

S. Geiger and K. S. Schmid, Institute of Petroleum Engineering, Heriot-Watt University, Riccarton Campus, Edinburgh EH14 4AS, UK. (sebastian.geiger@pet.hw.ac.uk; karen.schmid@pet.hw.ac.uk)